JOURNAL OF BAKU ENGINEERING UNIVERSITY - PHYSICS
2025. Volume 9, Number 2 *Pages 112-120*

UDC:539.219.3;358.931-405
DOI: **https://doi.org/10.30546/09081.2025.002.1034**

INFLUENCE OF Gd DOPING ON THE THERMOELECTRIC AND MAGNETO-TRANSPORT PROPERTIES OF SnSe

T.A.JAFAROV[1], O.M.HASANOV[1], J.I.HUSEYNOV[1], Kh.A.ADGOZALOVA[1], G.A.GARASHOVA[1], I.I.ABBASOV[2]

[1]*Azerbaijan State Pedagogical University*
AZ-1000, Baku, Uz. Hajibeyli Str.68, Baku, Azerbaijan
jahangirhuseynov1958@gmail.com
[2]*Azerbaijan State Oil and Industry University*
Az-1010, Baku, Azadlıq Avenue 20, Azerbaijan
ibrahimabbasov179@gmail.com

ARTICLE INFO

Article history:
Received:2025-06-01
Received in revised form:2025-06-16
Accepted:2025-07-02
Available online:2025-12-21

Keywords: $Gd_xSn_{1-x}Se$, layered crystals, thermoelectric properties, Nernst–Ettingshausen effect, rare earth elements, thermal conductivity, Hall coefficient, conductivity, doping, crystal lattice defects.

ABSTRACT

This work presents the results of synthesis and investigation of solid solutions in the $Gd_xSn_{1-x}Se$ system, obtained by direct melting followed by annealing. The phase composition, microstructure, kinetic parameters, as well as thermoelectric and thermomagnetic properties at various temperatures and magnetic fields were studied. It was found that the addition of gadolinium ions affects the type of conductivity, reduces the concentration and mobility of carriers, changes the Hall coefficients and thermoelectric power, and also enhances the longitudinal and transverse Nernst–Ettingshausen effects. The obtained data confirm the prospects of Gd-doped layered SnSe crystals for applications in thermoelectrics and sensor devices.

1. INTRODUCTION

Layered crystals are materials consisting of atomic layers held together by van der Waals forces. Due to their unique physicochemical properties and their intermediate position between molecular and nanostructures, they are considered promising nanomaterials [1, 2]. The properties of low-dimensional structures formed based on binary compounds depend on the type of chemical bonding and crystal structure [3, 4]. Binary compounds of the type $A^{IV}B^{VI}$ $(GeS, GeSe, SnS, SnSe)$ have anisotropic layered structures, which allow them to be exfoliated into atomically thin layers, similar to graphene. This makes them promising for $2D$ electronics and nanotechnologies [5, 6]. Low thermal conductivity and high anisotropy of electrical properties enhance their thermoelectric performance [7].

The addition of rare earth elements (REEs) into $SnSe$ leads to changes in electrophysical properties due to defect structures. REEs are characterized by low solubility and the ability to reduce background impurities [8, 9]. Doping improves conductivity, reduces thermal conductivity, and increases material stability, making it particularly suitable for thermoelectric applications [10, 11]. Thermomagnetic properties, which depend on temperature and magnetic field, are important for understanding charge carrier scattering mechanisms and developing

sensors, microelectronics, and energy systems [12–14]. These effects provide deeper insight into interactions in solids than carrier mobility alone.

In this regard, the synthesis and investigation of solid solutions based on $SnSe$ with Gd addition—a typical representative of REEs—are of interest. In this work, such solutions were obtained and their thermomagnetic properties, including the transverse and longitudinal Nernst–Ettingshausen effects, were studied.

2. EXPERIMENTAL SECTION

For the synthesis of $SnSe-GdSe$ alloys, tin of grade "B4-000", selenium "OC417-4", and chemically pure gadolinium (99.98%) were used. Synthesis was performed by a two-step direct melting method in evacuated quartz ampoules ($0.1333\ Pa$). At the first stage, the material was heated to the melting temperature of selenium at a rate of $4-5\ °C/min$ and held for $3-4\ hours$. Then the temperature was raised to $950-1000\ °C$ (depending on composition) and maintained for $8-9\ hours$. The resulting samples were annealed for $140-210\ hours$ in an argon atmosphere, with the annealing time increasing with higher Gd content [15].

Phase composition and physicochemical properties were studied using DTA, XRD, microstructural analysis, as well as microhardness and density measurements. DTA was performed on an STA 6000 instrument (Perkin Elmer, USA) in a nitrogen atmosphere ($20\ ml/s$) with heating up to the melting temperature at $5\ °C/min$. X-ray structural analysis was carried out on a Miniflex diffractometer (Rigaku) at $30\ kV, 10\ mA$, using $CuK\alpha$ radiation ($\lambda = 1.5406$ Å), in the 2θ range from 0 to 60°. Surface morphology was investigated using a JEOL JSM6610-LV scanning electron microscope.

Thermoelectric and thermomagnetic characteristics were measured by the steady-state compensation method. At temperatures of $300-620\ K$, thermoelectric power, as well as transverse (E_y) and longitudinal $(\Delta S/S_0)$ Nernst–Ettingshausen effects, were determined under a magnetic field of $11.000\ Oe$ [16]. Measurement errors were approximately 4.6% and 7.1%, respectively.

3. RESULTS AND DISCUSSION

Thermal analysis of the $Gd_xSn_{1-x}Se$ alloy system revealed no thermal anomalies other than the effect corresponding to melting. Substitution of part of the tin atoms in the binary $SnSe$ compound with terbium atoms leads to a decrease in the melting temperature. Analysis of the intensities of the $X-$ray reflections indicates the presence of a predominant crystallographic orientation and shows that the studied sample consists of a single phase. Indexing of the $X-$ray diffraction patterns demonstrates that, within the solubility range of Tb in $SnSe$, the investigated alloys crystallize in the orthorhombic system with space group $D_{2h}^{16}-Pcmn$ (Fig. 1). In the range $0 \le x \le 0.05$, no shifts of diffraction lines are observed, and only changes in their intensities indicate the formation of solid solutions based on $SnSe$. Changes in diffraction line intensities without their shifts confirm the formation of a substitutional solid solution within the Gd solubility range [17]. The lattice parameters increase linearly, consistent with Vegard's law.

The results of comprehensive physico-chemical analyses confirm that the $Gd_xSn_{1-x}Se$ alloy system, like the parent compound SnSe, crystallizes in the orthorhombic system. With

increasing TbSe concentration, a slight increase in unit cell parameters, density, and microhardness is observed, while thermal effects shift to relatively lower temperatures.

The introduction of Gd causes charge carrier scattering and an increase in unit cell parameters without significantly affecting density, indicating the formation of Frenkel-type defects [18]. It has been established that the solubility limit of Gd in $SnSe$ at room temperature does not exceed $2\ mol.\%$. Microstructure and physicochemical property studies confirm that with increasing $GdSe$ content, lattice parameters and microhardness increase, while thermal effects shift toward lower temperatures [19, 20].

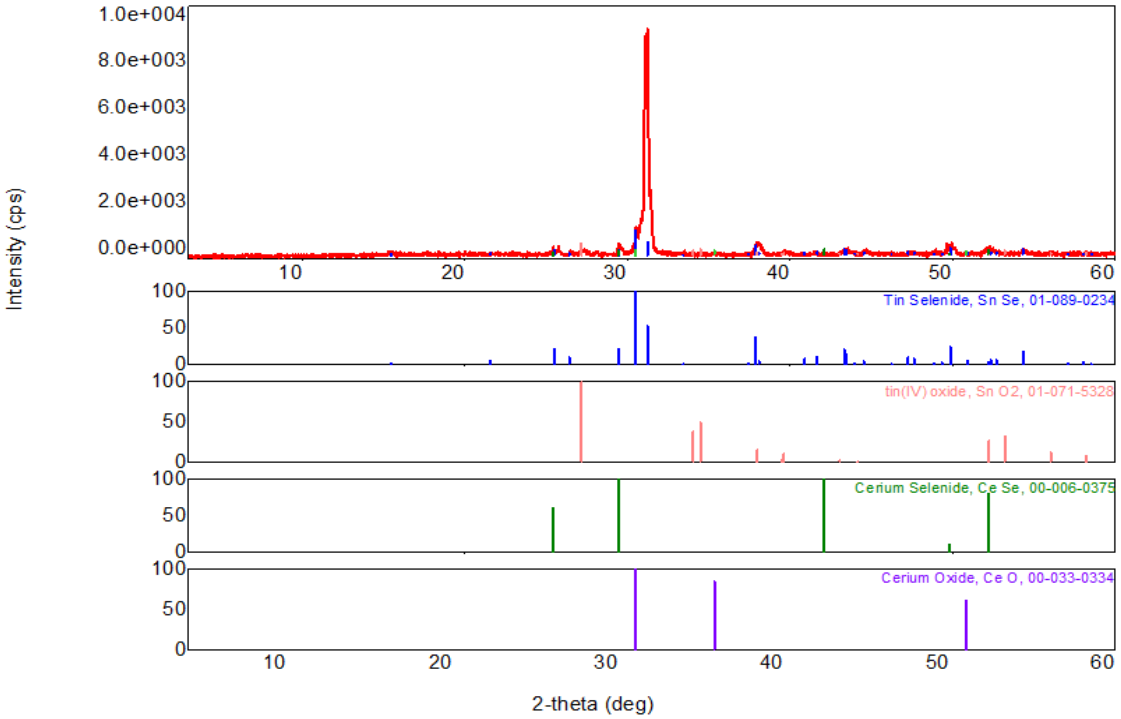

ray diffractograms of SnSe, SnO, GdSe and GdO compounds

Despite the layered nature of $SnSe$ single crystals, certain surface roughness is observed on the natural fracture surfaces (Fig. 2a). Atomic force microscopy (AFM) images show that the natural surface homogeneity of SnSe single crystals varies within approximately $25\ nm$ (Fig. 2b). This roughness is likely caused by the weakness of interlayer van der Waals interactions; when these bonds break, atomic clusters, rather than individual atoms, remain on the surface [21].

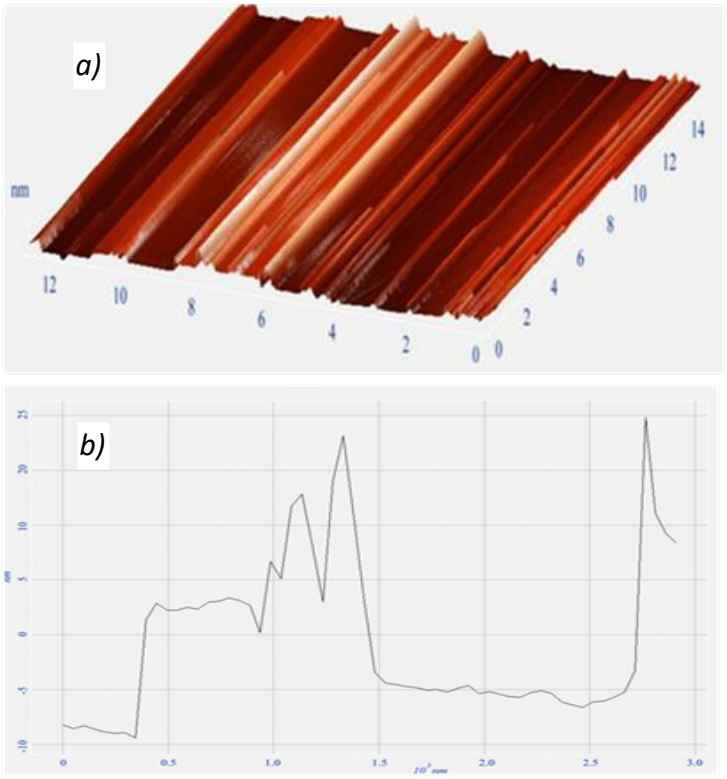

Figure 2. a) Surface roughness and b) surface profilogram of $Tb_xSn_{1-x}Se$ crystalsl

As the content of rare-earth metals (REMs) in $Gd_xSn_{1-x}Se$ single crystals increases, the surface roughness also increases. Partial substitution of tin atoms in the SnSe binary compound by REM atoms with larger atomic radii leads to enhanced interlayer van der Waals interactions. Therefore, with increasing Gd content in the $Gd_xSn_{1-x}Se$ alloy system, delamination along crystallographic planes becomes more difficult, resulting in increased surface inhomogeneity. This is also confirmed by Fourier spectra obtained via atomic force microscopy.

Quantitative X-ray microanalysis was used to determine the phase composition and the distribution of chemical elements on the surface of the studied sample. The analysis of the obtained results indicates surface homogeneity; however, changes in stoichiometry within the homogeneity region of $SnSe$ reveal a tendency toward selenium excess [22].

To more fully characterize the obtained compositions at room temperature, key kinetic parameters of the $Gd_xSn_{1-x}Se$ samples were measured: electrical conductivity (σ), Hall coefficient (R), thermoelectric power (S), and thermal conductivity (k). Based on these, charge carrier concentration ($p(n)$) and Hall mobility (μ) were calculated; the results are presented in the table below.

Table. *Main kinetic parameters of $Gd_xSn_{1-x}Se$ system alloys at T = 300K*

Sample compo-sition	σ $om^{-1}sm^{-1}$	R sm^3/Kl	S Vt/K	$10^{-3}\cdot$ k Vt/sm · K	μ $sm^2/V\cdot s$	p(n) sm^{-3}
x=0,0	76	2,105	405	18,7	160	$3\cdot 10^{18}$
x=0,0025	26	4,63	150	17, 36	120	$8.2\cdot 10^{17}$
x=0,005	5,43	9,88	297	16,21	54	$6.3\cdot 10^{17}$
x=0,01	4,32	-11, 14	-215	15,42	48	$5.6\cdot 10^{17}$
x=0,03	3,28	-13,42	-320	14,97	44	$5\cdot 10^{17}$

As seen from the table, with increasing Gd content, charge carrier concentration and their mobility sharply decrease. This is related to a change in the nature of the chemical bond: substitution of Sn^{2+} ions by Gd^{3+} strengthens the ionic component of the bond and reduces its directionality [23]. The additional positive charge of Gd^{3+} requires compensation, which may occur through the formation of point defects (e.g., selenium vacancies) that act as traps for carriers and reduce hole concentration. Additionally, Gd^{3+} can act as a donor, causing a transition from p-type to n-type conductivity or compensation thereof [24].

Differences in size and charge between Sn^{2+} and Gd^{3+} lead to local lattice distortions and enhanced carrier scattering, reducing their mobility. Formation of additional defects and clusters that intensify this scattering is also possible. Moreover, the reduction in thermal conductivity is due to phonon scattering on emerging structural disruptions and alloy disorder [25].

The temperature dependence of thermoelectric power in $Gd_xSn_{1-x}Se$ solid solutions is shown in Fig. 3. Its behavior is related to electronic structure features and carrier transport mechanisms. Upon gadolinium addition to $p-SnSe$, both the magnitude and sign of thermoelectric power change [26].

In the sample with $x = 0.0025$, $S(T)$ increases from 60 to $250\ \mu V/K$ in the range $100-450\ K$, then decreases. This is associated with an increase in thermally excited carrier concentration and subsequent generation of electron-hole pairs compensating the thermoelectric contribution. At Gd content $\geq 0.005\ at.\%$, a conductivity type change is observed. For the $x = 0.005$ sample at $T = 420\ K$, the sign of S inverts from positive to negative, indicating a transition from $p-$ to $n-$type conduction. In samples with $x > 0.005$, this transition occurs at higher temperatures (e.g., $T = 500\ K$ for $x = 0.03$).

In all solid solutions, thermoelectric power first increases and then decreases with temperature, explained by a two-band model with light and heavy holes. Hall coefficients and thermoelectric power correlate well, confirming the complexity of the band structure [27]. Thermoelectric power in pure $SnSe$ is higher in all temperature ranges than in doped samples. Substitution of Sn with rare-earth elements reduces S and shifts the region of its decrease toward higher temperatures.

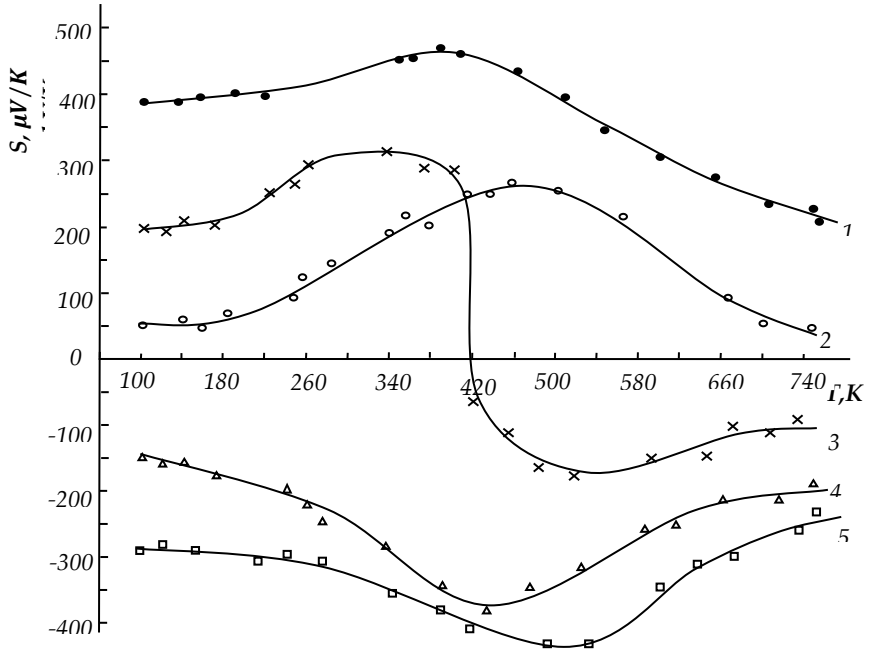

Figure 3. *Temperature dependence of thermo-EMF in system $Gd_xSn_{1-x}Se$ crystals:1-x =0; 2-x=0.0025; 3-0.005 4-x=0.01; 5-x=0.03*

Fig. 4 shows the temperature dependence of the Nernst–Ettingshausen transverse effect coefficient (E_y) for $Gd_xSn_{1-x}Se$ alloys with different gadolinium contents: $x = 0$ (sample No.1), 0.0025 (No.2), and 0.01 (No.4). In pure $SnSe$ (curve 1) in the range $100–450\ K$, E_y rises from 5.8% to 9%, then gradually decreases at $460–740\ K$ but remains positive. This behavior is associated with an increase in carrier concentration and mobility upon heating, followed by enhanced scattering [28].

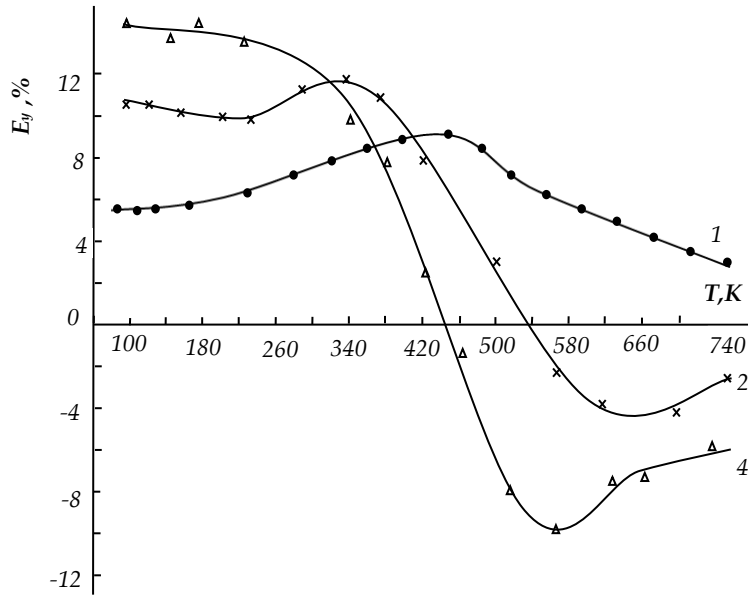

Figure 4. *Temperature dependence of the transverse N-E effect in some compositions of $Gd_xSn_{1-x}Se$ crystals: 1-x=0.0; 2 - x = 0.0025; 4 - x = 0.01*

In doped alloys, the character of E_y dependence changes. In sample No.2 with $x = 0.0025$, a maximum is observed near $380\ K$, after which the coefficient decreases and changes sign to negative at $540\ K$, indicating a change in the dominant carrier type. This is related to the activation of heavy holes and influence of local levels introduced by Gd^{3+}.

For sample No.4 ($x = 0.01$), the effect becomes negative already at $430\ K$, with a maximum (in absolute value) around $550–560\ K$. With increasing Gd content, the inversion temperature shifts to higher values. This is explained by the donor nature of Gd^{3+} and Fermi level shift, leading to an earlier disruption of electron-hole balance.

Fig. 5 presents the dependencies of thermoelectric power change ($\Delta S(H)$) on magnetic field for $Gd_xSn_{1-x}Se$ alloys at various temperatures. At $95\ K$, a more pronounced growth of $\Delta S(H)$ up to $6\ kOe$ is observed, after which the increase slows. The dependence is nonlinear and does not reach saturation. At $310\ K$, the curve approaches linearity.

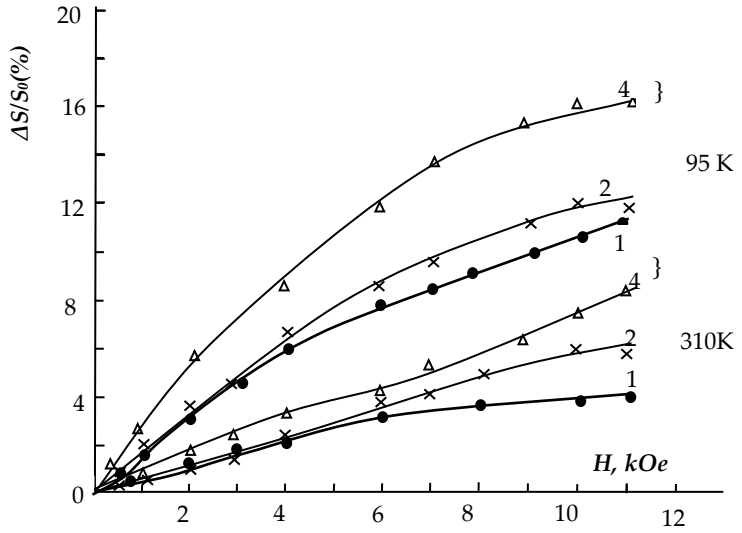

Figure 5. *The dependence of ΔS on the magnetic field(H) in $Gd_xSn_{1-x}Se$ crystals: 1-x=0.0; 2 - x = 0.0025; 4 - x = 0.01*

With increasing gadolinium content, $\Delta S(H)$ increases, indicating enhancement of the longitudinal Nernst–Ettingshausen effect. At low temperatures, weakened thermal vibrations make carriers more sensitive to the magnetic field, and nonlinearity reflects a change in dominant mechanisms. At high temperatures, thermal scattering predominates, reducing magnetic field influence. The more pronounced effect in samples with high Gd content is explained by additional magnetic scattering and the influence of rare-earth ions on the electronic structure.

4. CONCLUSION

This work presents the results of synthesis and comprehensive investigation of $Gd_xSn_{1-x}Se$ solid solutions obtained by the direct melting method. It was established that the introduction of Gd^{3+} ions into the $SnSe$ crystal lattice leads to the formation of a substitutional solid solution, accompanied by an increase in lattice parameters, an increase in microhardness, and a decrease in the melting temperature. The studies showed that the addition of Gd significantly affects the electrophysical and thermomagnetic properties of the materials. A decrease in carrier

concentration and mobility was observed, along with an inversion of the sign of the thermoelectric power and the Nernst–Ettingshausen coefficient, as well as an enhancement of the longitudinal N–E effect in a magnetic field. These phenomena are explained by the formation of point defects, a change in the type of conductivity, and enhanced carrier scattering. The obtained results confirm the potential of doping SnSe with rare-earth elements to control its physical properties and to improve its efficiency in thermoelectric and sensor applications.

REFERENCE

1. Duong D.L. , Yun S.J. , Lee Y.H. (2017) van der Waals Layered Materials: Opportunities and Challenges. ACS Nano , 11 (12), 11803–11830; https://doi.org/10.1021/acsnano.7b07436
2. Kim J., Song O., Cho Y.S., Jung M., Rhee D., Kang J. (2022) Revisiting Solution-Based Processing of van der Waals Layered Materials for Electronics. ACS Materials Au, 2 (4), 382–393; https://doi.org/10.1021/acsmaterialsau.2c00034
3. Stepanov R.S., Marland P.I., Kolobov A.V. (2023) Compositional and Structural Disorder in Two-Dimensional $A^{III}B^{VI}$ Materials. *Crystals, 13 (*8), 1209;
4. https://doi.org/10.3390/cryst13081209
5. Dede D., Morgan N., Gächter N., Nurmamytov T. , Luca M.D. et al. (2022) Low Dimensional III-V and II-VI Semiconductors. Microscopy and Microanalysis, 28 (S1), 2004; http://dx.doi.org/10.1017/s1431927622007784.
6. Buruiana A.-T., Mihai C., Kuncser V., Velea A. (2025) Advances in 2D Group IV Monochalcogenides: Synthesis, Properties, and Applications. *Materials*, *18* (7), 1530; https://doi.org/10.3390/ma18071530
7. Guo S.-D. , Wang Y.-H. (2017) Thermoelectric properties of orthorhombic group IV–VI monolayers from the first-principles calculations. J. Appl. Phys. 121, 034302; https://doi.org/10.1063/1.4974200
8. Ding G. , Gao G. , Yao K. (2015) High-efficient thermoelectric materials: The case of orthorhombic IV-VI compounds. Scientific Reports, 5, 9567; https://doi.org/10.48550/arXiv.1505.02477
9. Isber S., Gratens X. (2010) Crystal growth and magnetic properties of tin selenide-doped europium $Sn_{1-x}Eu_xSe$. Journal of Magnetism and Magnetic Materials. 322, 1113–1116.
10. Wei B., Zhang J., Lin L., Wu T., Cheng Z., Ma Y., Li J., Yu S. (2024) Enhancing Electrical Transport Performance of Polycrystalline Tin Selenide by Doping Different Elements. Physica Status Solidi (A) Applications and Materials. Vol. 221, Is. 9, 2300717; https://doi.org/10.1002/pssa.202300717
11. Yang X., Ma X-Y., Shi T.-E., Bao W-Q., Wang J., et al. (2024) High thermoelectric properties in polycrystalline SnSe materials realized by rare earth halide Co-doping. Ceramics International, Vol. 50 (11), Part B, pp. 20515-20524;
12. https://doi.org/10.1016/j.ceramint.2024.03.173
13. Li S., Yin Li, Liu Y., Wang X., Chen C., Zhang Q. (2023) Rare earth element Ce enables high thermoelectric performance in n-type SnSe polycrystals. Journal of Materials Science & Technology. 143, 234-24120; https://doi.org/10.1016/j.jmst.2022.09.054
14. Askerov B. M. (1994) Electron Transport Phenomena in Semiconductors. World Scientific, Singapore, New Jersey, London, 394 p.
15. Yamada R., Nomoto T., Miyake A., Terakawa T., Kikkawa A., et al. (2024) Nernst Effect of High-Mobility Weyl Electrons in NdAlSi Enhanced by a Fermi Surface Nesting Instability. Physical Review X. 14, 021012; DOI: 10.1103/PhysRevX.14.021012
16. Akhanda S., Schlaak K.A., Scott E.F., Taj N.A., Watzman S. J., Zebarjadi M. (2024) Thermomagnetic responses of semimetals. *J. Appl. Phys.* 135, 240901;
17. https://doi.org/10.1063/5.0192824
18. Huseynov J.I., Murguzov M.I., Ismayilov S.S. (2013) Specificfeatures of self-compensation in $Er_xSn_{1-x}Se$ solid solutions Semiconductors 47, 323–326;
19. https://doi.org/10.1134/S106378261303010X
20. Huseynov J.I., Murguzov M.I., Ismayilov S.S., et al. (2017) On the thermopower and thermomagnetic properties of $Er_xSn_{1-x}Se$ solid solutions. Semiconductors 51, 153–157; https://doi.org/10.1134/S1063782617020075

21. Aliev I.I. , Huseynov J.I. , Murguzov M.I. , Ismailov Sh.S. , Gojaev E.M. (2014) Phase relations and properties of alloys in the SnSe-DySe system. Inorg Mater, 50, 237–240; https://doi.org/10.1134/S0020168514030029
22. Ismailov Sh.S., Huseynov J.I., Musaev M.A., Abbasov I.I., Abdurakhmanova V.A. (2020) Effect of doping level and compensation on thermal conductivity in $Ce_xSn_{1-x}Se$ solid solutions *Low Temp. Phys.* 46, 1114–1120; https://doi.org/10.1063/10.0002155
23. Abbasov I.I., Ismailov Sh.S., Huseynov J.I., Abdurakhmanova V.A. (2019) Concentration dependences of electrical conductivity and the Hall effect of the $Ce_xSn_{1-x}Se$ single crystals. *Low Temp. Phys.* 45, 1277–1280; https://doi.org/10.1063/10.0000209
24. J.I.Hüseynov, Kh.A.Hasanov, T.A.Jafarov, I.I.Abbasov.(2020) Compensating effect of terbium impurity on the conductivity of $Tb_xSn_{1-x}Se$ solid solutions. Ukrainian journal of physics. 65 (3), 225-230; http://jnas.nbuv.gov.ua/article/UJRN-0001127989
25. Jagani H.S., Dixit V., Patel A., Gohil J., Pathak V.M. (2022) Stability & durability of self-driven photo-detective parameters based on $Sn_{1-\beta}Sb_\beta Se$ (β = 0, 0.05, 0.10, 0.15, 0.20) ternary alloy single crystals. RSC Adv., 12 (44), 28693-28706; DOI:10.1039/D2RA05492
26. Abbasov I.I., Musayev M.A., Huseynov C.I., Eyyubov Q.Y., Hasimova N.N., Mammadova A.J. (2023). A study of impurity defect photoluminescence in ZnSe: Cr and ZnSe: Fe in the near infrared at room temperature. Advanced Physical Research, 5 (3), 192-199
27. Hu H., Su B., Liu X., Thong H-C., Jiang Y., et al. (2024) Chemical bond engineering toward extraordinary power factor and service stability in thermoelectric copper selenide. Joule, 8, 416–429; doi.org/10.1016/j.joule.2023.12.019
28. Abbasov I.I., Huseynov J.I. (2017) Charge-transfer processes in $(SnS)_{1-x}(PrS)_x$ Alloys. Ukrainian journal of physics. 62 (10), 883-888; http://jnas.nbuv.gov.ua/article/UJRN-0000795750
29. Dhahri R., Benamara M., Bouzidi S., Moussa S.B., Abdullah A.Y., et al. (2025) Effect of Gd doping on the microstructure and electrical characteristics of Maghemite (γ-Fe_2O_3) ceramics. J Sol-Gel Sci Technol. 113, 225–242; https://doi.org/10.1007/s10971-024-06598-0
30. Huseynov D.I., Murguzov M.I., Ismailov S.S. (2008) Thermal conductivity of $Er_xSn_{1-x}Se$ ($x \leq 0.025$) solid solutions. Inorg Mater 44, 467–469;
31. https://doi.org/10.1134/S0020168508050063
32. Hasanov K.A., Huseynov J.I., Dadashova V.V., Aliyev F.F. (2016) Effect of Phonon Drag on the Thermopower in a Parabolic Quantum Well. Semiconductors 50, 295–298 https://doi.org/10.1134/S106378261603009X
33. Hasanov O.M., Huseynov C.I., Aslanov H.A., Adgozalova X.A., Garashova G.A., Bayramli R.B., (2024) Galvanomagnetic properties of $Gd_xSn_{1-x}Se$ solid solutions. Journal of Baku Engineering university – Physics, 8, 2, 81-90, https://doi.org/10.30546/09081.2024.102.7068
34. Huseynov J.I., Jafarov T.A., Hasanov O.M., Adgezalova Kh.A., (2019). Thermoelectric and thermomagnetic properties of the $Tb_xSn_{1-x}Se$ alloy systems. Applied physics 6, 82; https://applphys.orion-ir.ru/appl-19/19-6/PF-19-6-82.pdf